DOI: 10.1002/chem.201201197

A Small-Molecule Two-Photon Probe for Nitric Oxide in Living Tissues

Eun Won Seo,[a] Ji Hee Han,[b] Cheol Ho Heo,[a] Jae Ho Shin,[c] Hwan Myung Kim,*[a] and Bong Rae Cho*[b]

Abstract: Two-photon microscopy (TPM) has become an indispensable tool in the study of biology and medicine due to the capability of this method for molecular imaging deep inside intact tissues. For the maximum utilization of TPM, a variety of two-photon (TP) probes for specific applications are needed. In this article, we report a small-molecule TP probe (ANO1) for nitric oxide (NO) that shows a rapid and specific NO response, a 68-fold fluorescence enhancement in response to NO, and a maximum TP-action cross-section of 170 GM (GM: 10^{-50} cm^4 $photon^{-1}$) upon reaction with excess NO. This probe can be easily loaded into cells and tissues and can real-time monitor NO in living tissues at 100–180 μm depth for longer than 1200 s through the use of TPM, with minimum interference from other biologically relevant species.

Keywords: fluorescent probes · living tissues · nitrogen oxides · two-photon microscopy · two-photon probe

Introduction

Small-molecule-derived fluorescent probes are essential tools for studying cell biology such as small-molecule signaling.[1–5] Nitric oxide (NO) is a ubiquitous signaling molecule that modulates a variety of physiological and pathological processes in living organisms. NO plays a key role in synaptic activity in the brain and defends immune systems. On the other hand, misregulation of NO production can cause various diseases, such as cancer and neurodegenerative disorders.[6–10] In order to understand its roles in biology, it is crucial to monitor NO in intact tissues.

To detect NO in live cells, a number of fluorescent probes derived from *o*-diaminobenzene have been developed, with diaminofluoresceins such as 4,5-diaminofluorescein (DAF-2) being commercially available.[11–14] It is well accepted that the *o*-diaminobenzene moiety in these probes is converted into triazine by reaction with the autooxidation products of NO such as NO^+ and N_2O_3, thereby blocking the photoinduced electron transfer (PeT) and allowing strong emission.[11–14] Lippard's group reported a Cu^{II}–fluorescein-based probe (CuFL) with a much faster response, which was useful for real-time imaging of NO in live cells.[15–17] More recently, a reaction-based turn-on probe has been developed to detect NO in live cells.[18] These small-molecule probes do not require transfection, unlike their protein counterparts.[19–21] However, the use of these probes with one-photon microscopy (OPM) requires rather short excitation wavelengths (< 500 nm), which limits their application in tissue imaging due to the shallow penetration depth (< 80 μm). Nagano and co-workers reported a cyanine-derived NO probe for near-infrared (NIR) microscopy imaging.[14] Although NIR microscopy is useful for imaging big objects such as a whole mouse, it is not suitable for imaging microlevel objects, such as cells and tissue slices, with high resolution. Two-photon microscopy (TPM) overcomes these problems. TPM, which employs two near-infrared photons as the excitation source, offers a number of advantages over one-photon microscopy, including increased depth of penetration (> 500 μm), localized excitation, and prolonged observation times.[22,23] In this context, TPM has become indispensable to the study of biology and medicine due to its capability for molecular imaging deep inside intact tissues with minimum interference from background emissions and minimum photodamage.[24–26] However, to the best of our knowledge, there has been no report of a two-photon (TP) probe for NO that is applicable for deep-tissue imaging. We therefore designed a simple and efficient TP turn-on probe (ANO1, Scheme 1) by considering the following requirements: 1) a low molecular weight for cell permeability,[27] 2) an appreciable water solubility to stain the cells and tis-

[a] E. W. Seo,[+] C. H. Heo, Prof. Dr. H. M. Kim
Division of Energy Systems Research
Ajou University
Suwon, 443-749 (Korea)
Fax: (+82) 31-219-1615
E-mail: kimhm@ajou.ac.kr

[b] J. H. Han,[+] Prof. Dr. B. R. Cho
Department of Chemistry
Korea University
1-Anamdong, Seoul, 136-701 (Korea)
Fax: (+82) 2-3290-3544
E-mail: chobr@korea.ac.kr

[c] Prof. Dr. J. H. Shin
Department of Chemistry
Kwangwoon University
Seoul, 139-701 (Korea)

[+] These authors contributed equally to this work.

Supporting information for this article is available on the WWW under http://dx.doi.org/10.1002/chem.201201197.

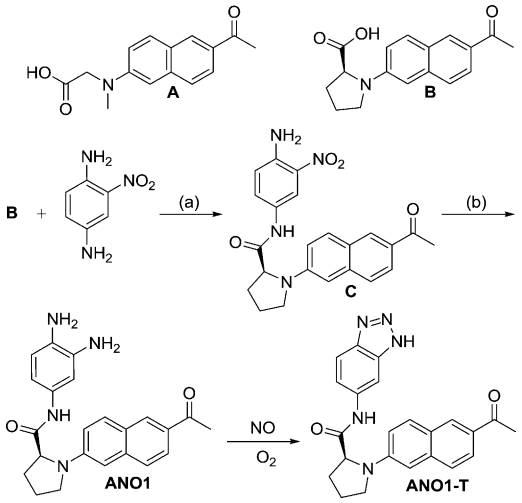

Scheme 1. Synthesis of ANO1 and ANO1-T: a) DCC, HOBt, CH_2Cl_2, b) $SnCl_2{\cdot}2H_2O$, CH_2Cl_2. DCC: 1,3-dicyclohexylcarbodiimide; HOBt: 1-hydroxy-1*H*-benzotriazole.

sues,[28] 3) a high selectivity for NO, 4) a large turn-on response for superior spatial resolution,[29] 5) a significant TP cross-section for a bright TPM image, and 6) high photostability.

In this article, we present the design, synthesis, spectroscopic properties in both one- and two-photon mode, and TPM-imaging application of ANO1, which can detect nitric oxide in live cells and intact tissues for a long period of time through the use of TPM.

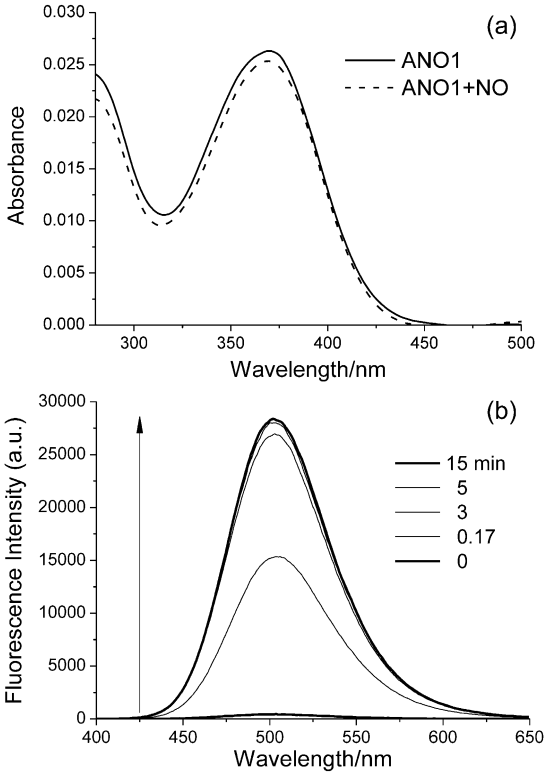

Figure 1. a) One-photon absorption spectra of ANO1 (2 μM) after addition of 100 μM NO in PBS (pH 7.4). Spectra were acquired in PBS (pH 7.4) at 0 and 15 min after addition of NO. b) One-photon fluorescence response with time for the reaction of ANO1 (2 μM) with NO (100 μM) at 37 °C. Spectra were acquired in PBS (pH 7.4) between 0 and 15 min after addition of NO. Excitation at $\lambda = 370$ nm.

Results and Discussion

It has been well established that the combination of a receptor for the target species and a 2-acetyl-6-dialkylaminonaphthalene (acedan) as the reporter with a glycinamide linkage is a simple and effective strategy to design a TP turn-on probe.[30–32] We have now developed an efficient TP probe for NO based on an acedan as the reporter and an *o*-diaminobenzene as the reaction site for NO, linked by prolinamide (ANO1, Scheme 1), with the expectation that the TP excited-fluorescence (TPEF) intensity would increase dramatically upon reaction with NO.[29] The acedan was adopted from our earlier work[30,31] and the *o*-diaminobenzene from the work of Nagano and co-workers.[12–14] ANO1 was prepared in 35% yield by the coupling of **B** and 2-nitro-1,4-phenylenediamine followed by reduction (Scheme 1 and see the Experimental Section). The reaction between ANO1 and NO, as monitored by fluorescence emissions (Figure 1b) and LC-MS (Figure S1 in the Supporting Information), produced ANO1-T as the only major product.

The solubility of ANO1 and ANO1-T in phosphate-buffered saline (PBS; 30 mM, containing 100 mM KCl, pH 7.4) as determined by the fluorescence method is 4 μM,[28] which is sufficient to stain cells (Figure S2 in the Supporting Information). Under these simulated physiological conditions, ANO1 exhibits an absorption maximum at $\lambda_{abs} = 370$ nm (extinction coefficient: $\varepsilon = 12\,700\ M^{-1}cm^{-1}$) and a fluorescence maximum at $\lambda_{fl} = 502$ nm (fluorescence quantum yield: $\Phi = 0.009$). The emission spectra of ANO1 showed gradual redshifts with increasing solvent polarity in the order 1,4-dioxane < *N*,*N*-dimethylformamide (DMF) < EtOH < buffer (Figure S3 and Table S1 in the Supporting Information). The large redshifts (>85 nm) with increasing solvent polarity indicate the utility of ANO1 as an environment-sensitive probe.

When excess NO was added to ANO1 in PBS, the fluorescence intensity ($FEF = F_{max}/F_{min}$) increased 68-fold within 5 min without affecting the absorption spectra, presumably due to blocking of the PeT upon oxidation (Figure 1). The large turn-on response is consistent with a 78-fold higher fluorescence quantum efficiency ($\Phi = 0.70$, Table 1) of ANO1-T than that of ANO1. Moreover, the plot of the fluorescence intensity against the NO concentration was linear in the range from 5 nM to 20 μM (Figure S4 in the Supporting Information), which indicates that ANO1 can detect NO at concentrations as low as 5 nM.

ANO1 showed high selectivity for NO over competing reactive nitrogen and oxygen species (RNS, ROS), including nitroxyl (HNO), nitrite (NO_2^-), nitrate (NO_3^-), hydrogen peroxide (H_2O_2), peroxynitrite ($ONOO^-$), *tert*-butylhydro-

Table 1. Photophysical data for compounds **A**, **B**, ANO1, and ANO1-T.[a]

	$\lambda_{max}^{(1)}$ (10^{-4} ε) [nm][b]	λ_{max}^{fl} [nm][c]	Φ[d]	$\lambda_{max}^{(2)}$ [nm][e]	$\Phi\delta_{max}$ [GM][f]
A	380 (1.24)	515	0.34	750	55
B	385 (1.44)	520	0.55	750	100
ANO1	370 (1.27)	502	0.009	750	n.d.[g]
ANO1-T	370 (1.22)	502	0.70	750	170

[a] All measurements were performed in PBS. [b] λ_{max} value of the one-photon absorption spectra. The numbers in parentheses are the molar extinction coefficients in $M^{-1}cm^{-1}$. [c] λ_{max} value of the one-photon emission spectra. [d] Fluorescence quantum yield. [e] λ_{max} value of the two-photon excitation spectra. [f] The peak two-photon-action cross-section (GM: 10^{-50} cm^4 $photon^{-1}$). [g] n.d.: not determined. The TPEF intensity was too weak to measure the cross-section accurately.

peroxide (TBHP), hypochlorite (OCl^-), superoxide ($O_2^{\cdot-}$), singlet oxygen ($^1O_2$), hydroxyl radical ($^{\cdot}OH$), and *tert*-butoxy radical ($^{\cdot}OtBu$), as well as ascorbic acid (AA) and dehydroascorbic acid (DHA) (Figure 2a). The high selectivity over AA and DHA is particularly interesting for biological applications because DAF-2 does not show such selectivity.[33,34] It is well known that the fluorophore part can affect the binding affinity of the probe, so this outcome might be

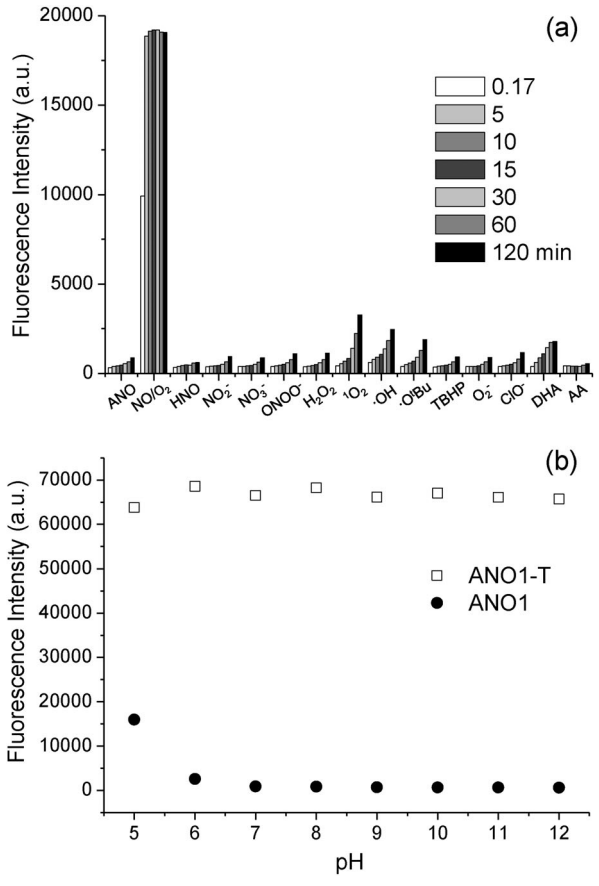

Figure 2. a) Fluorescence responses of 2 μM ANO1 to various reactive oxygen and nitrogen species (100 μM) and to AA and DHA (1 mM). b) Effect of the pH value on the one-photon fluorescence intensity of 2 μM ANO1 (●) and ANO1-T (□) in universal buffer (0.1 M citric acid, 0.1 M KH_2PO_4, 0.1 M $Na_2B_4O_7$, 0.1 M tris(hydroxymethyl)aminomethane (Tris), 0.1 M KCl). Excitation at $\lambda = 370$ nm.

due to the different structures of ANO1 and DAF-2.[35] Moreover, the fluorescence response decreased significantly under deoxygenated conditions, thereby confirming that the oxidized form of NO is responsible for the detection (Figure S5 in the Supporting Information).[11–14] Furthermore, ANO1 and ANO1-T are pH insensitive in the biologically relevant pH range (Figure 2b). The combined results reveal that ANO1 can detect NO under physiological conditions with minimum interference from other RNS, ROS, AA, and DHA, as well as from the pH value.

We then evaluated the ability of ANO1 to detect NO in a two-photon mode. The TP-action cross-section was determined by investigating the TPEF spectra of ANO1 and ANO1-T with rhodamine-6G as the reference (see the Experimental Section). Whereas the peak TP-action cross-section ($\Phi\delta_{max}$) of ANO1 in PBS was too small to measure accurately, that of ANO1-T was 170 GM at 750 nm under the same conditions (Table 1 and Figure 3; GM: 10^{-50} cm^4 $photon^{-1}$). This predicts a very large TP turn-on response upon NO-induced ANO1-T formation, as observed in the one-photon experiment (see above). These results allowed us to detect NO in cells and tissues labeled with ANO1. Moreover, the $\Phi\delta_{max}$ value of ANO1-T is significantly larger than those of other **A**-derived TP probes, despite their similar structures.[30,31] This outcome could be explained with the photophysical properties of **A** and **B**. As shown in Table 1, the Φ and $\Phi\delta_{max}$ values are both larger for **B** than for **A** by 1.8-fold, which indicates that the larger $\Phi\delta_{max}$ value of **B** is due to the larger Φ value. The cyclic structure of the proline moiety may have reduced the vibrational relaxation pathways, thereby increasing the Φ and $\Phi\delta_{max}$ values. This result underlines the advantage of introducing prolinamide as the donor and linker in the design of TP turn-on probes.

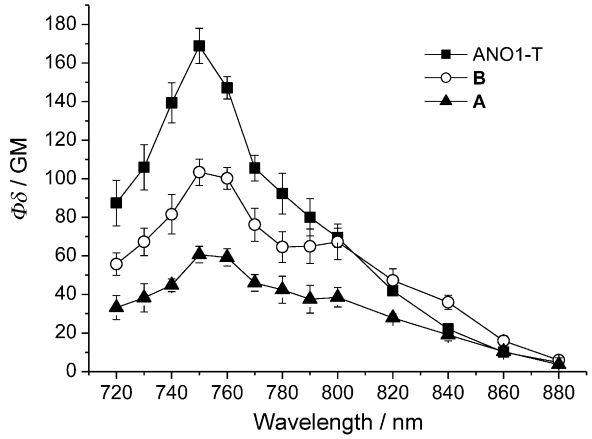

Figure 3. Two-photon-action spectra of 1 μM **A**, **B**, and ANO1-T in PBS (pH 7.4). The estimated uncertainties for the TP-action cross-section values ($\Phi\delta$) are ±15%.

The TPEF spectrum from ANO1-labeled Raw 264.7 murine macrophage cells was symmetrical and slightly blue-shifted ($\lambda_{fl} = 490$ nm) relative to that measured in PBS (Fig-

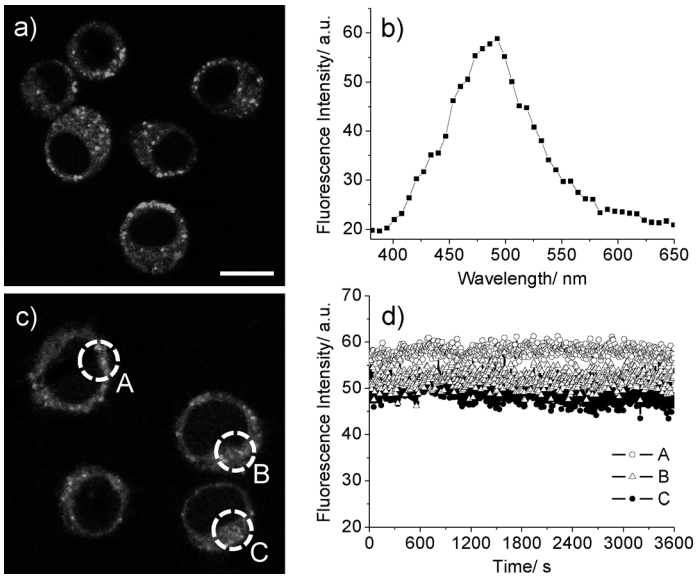

Figure 4. a, c) TPM images of ANO1-labeled (3 μM) Raw 264.7 cells. b) Two-photon excited-fluorescence spectrum measured from (a). d) The relative TPEF intensity from the marked areas A–C in (c) as a function of time. The digitized intensity was recorded with 1.63 s intervals for the duration of 1 h by using *xyt* mode. The TPEF intensities were collected at 425–575 nm upon excitation at 750 nm with fs pulses. Cells shown are representative images from replicate experiments ($n=5$). Scale bar: 20 μm.

ure 4 b). This indicates that the polarity of the probe environment is rather homogeneous and slightly more hydrophobic than that of the PBS. Therefore, we detected the TPEF by using a detection window of 425–575 nm. Also, the TPEF intensity at a given spot on the ANO1-labeled cells remained nearly the same after continuous irradiation with the fs pulses for 60 min, which indicated the high photostability of the ANO1 (Figure 4 d).

Next, we tested the ability of ANO1 to detect NO in the cells. The TPM image of Raw 264.7 cells labeled with ANO1 was bright (Figure 4 and Figure 5). The fluorescence intensity of ANO1 increases slightly at pH < 5 in the universal buffer, so there is a possibility that the probe being located in acidic compartments might be responsible for the bright image. To assess such a possibility, Raw 264.7 cells were co-labeled with ANO1 and LysoTracker Red (LTR),[36] a well-known OP probe for acidic vesicles, and the TPM image was colocalized with the OPM image (Figure 5 a–c and Figure S6 in the Supporting Information). The Pearson's colocalization coefficient (A), which describes the correlation of the intensity distribution between the channels,[37] was calculated by using Autoquant X2 software. The A value of ANO1 with LTR was 0.18 (Figure 5 c). This indicates that ANO1 is partially localized in the acidic compartments. Moreover, when the cells were pretreated with bacterial lipopolysaccharide (LPS) and interferon-γ (IFN-γ), which are well-known external activators that promote NO production by inducible nitric oxide synthase (iNOS),[9] the TPEF intensity increased abruptly (Figure 5 d, e). The average TPEF intensity lies between those measured in ANO1- and ANO1-T-labeled cells (Figure 5 h). Moreover, the increase was suppressed by addition of L-N^G-nitroarginine (L-NNA), an iNOS inhibitor,[38] which confirmed that the bright signals in the TPM images reflect

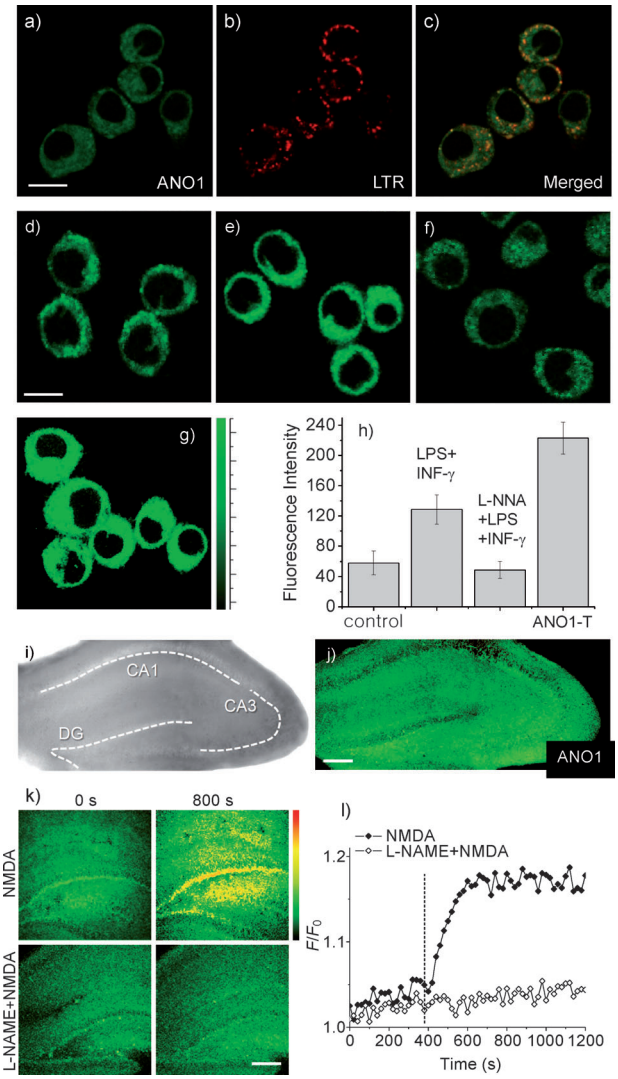

Figure 5. a) TPM images of ANO1-labeled (3 μM) Raw 264.7 cells collected at 425–525 nm. b) OPM image of LTR-labeled macrophages collected at 575–660 nm. c) Co-localized image of (a) and (b). d and g) TPM images of Raw 264.7 cells labeled with d) 3 μM ANO1 and g) 3 μM ANO1-T, respectively, for 30 min. e) Cells were pretreated with 1.25 μg mL^{-1} LPS and 200 U mL^{-1} IFN-γ for 9 h and then incubated with ANO1 for 30 min. f) Cells were pretreated with 10 μM L-NNA, 1.25 μg mL^{-1} LPS, and 200 U mL^{-1} IFN-γ for 9 h and then incubated with ANO1 for 30 min. Cells shown are representative images from replicate experiments ($n=5$). h) Average TPEF intensities in (d)–(g). Images of a rat hippocampal slice stained with 20 μM ANO1: i) Bright-field image of the CA1 and CA3 regions, as well as the dentate gyrus (DG), with 10× magnification. j) TPM image with 10× magnification. 25 TPM images were accumulated along the z direction at depths of approximately 100–180 μm. k) Magnification at 40× in the DG region at a depth of approximately 100 μm before and after addition of 1 mM NMDA or 100 μM L-NAME and 1 mM NMDA to the imaging solution. l) Time course of the TPEF intensity in (k). (d)–(l) The TPEF data were collected at 425–575 nm upon excitation at 750 nm with fs pulses. Scale bars: a, d) 20, j) 300, and k) 75 μm.

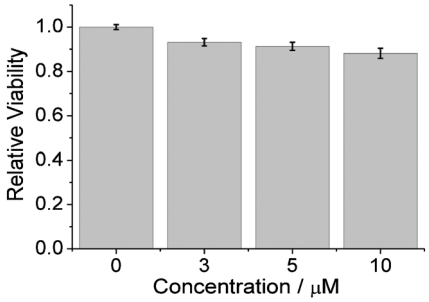

Figure 6. Viability of Raw 264.7 cells in the presence of ANO1 as measured by using a CCK-8 kit. The cells were incubated with 0, 3, 5, and 10 μM ANO1 for 6 h.

the presence of NO (Figure 5f,h). Furthermore, ANO1 was found to be nontoxic to cells during the imaging experiments, as determined by using a Cell Counting Kit 8 (CCK-8) assay (Figure 6). These results establish that ANO1 is capable of detecting NO in living cells with minimum interference from pH value and cytotoxicity.

We further investigated the utility of ANO1 in live-tissue imaging. TPM images were obtained from a slice of 14-day-old rat hippocampal tissue incubated with 20 μM ANO1 for 1 h at 37 °C. It takes a longer time to stain the living tissues, during which time they may be deformed, so an excess amount (20 μM) of ANO1 was used to facilitate staining. The slice from the brain was too large to show with one image, so two images were obtained in each *xy* plane and combined. The bright-field image revealed the CA1 and CA3 regions and also the dentate gyrus (DG; Figure 5i). As the structure of the brain tissue is known to be inhomogeneous in its entire depth, we accumulated ten TPM images at depths of 100–180 μm to visualize the distribution of NO. They reveal intense fluorescence in the DG and CA3 regions (Figure 5j).[39] The image obtained at a higher magnification clearly shows the distribution of NO in the DG region (Figure 5k). When 1 mM *N*-methyl-D-aspartic acid (NMDA), a reagent that promotes NO production by constitutive nitric oxide synthase (cNOS),[39,40] was added to the imaging solution, the TPEF intensities increased immediately. Moreover, the increase was suppressed by the addition of *N*-(G)-nitro-L-arginine methyl ester (L-NAME), a cNOS inhibitor,[39,40] which confirmed that the bright signals in the TPM images reflect the presence of NO (Figure 5k,l). Furthermore, the TPM images obtained at a depth of 100–180 μm revealed the NO distribution in the given plane along the *z* direction in the CA1 and DG regions (Figure S7 in the Supporting Information). These findings demonstrate that ANO1 is capable of detecting NO at a depth of 100–180 μm in living tissues by using TPM.

Conclusion

We have developed a small-molecule TP turn-on probe (ANO1) that shows a rapid and specific NO response, pH insensitivity in the biologically relevant range, strong TPEF enhancement in response to NO, and a maximum TP-action cross-section of 170 GM upon reaction with excess NO. This probe can be easily loaded into cells and can real-time monitor the NO in living tissues at 100–180 μm depth for a long period of time with minimum interference from other biologically relevant species through the use of TPM.

Experimental Section

Synthesis of ANO1 and ANO1-T: Compound **B** was prepared by the literature method,[29] and the synthesis of the other compounds is described below.

*Synthesis of **C***: Compound **B** (0.38 g, 1.34 mmol), 2-nitro-1,4-phenylenediamine (0.17 g, 1.12 mmol), 1,3-dicyclohexylcarbodiimide (DCC, 0.29 g, 1.40 mmol), and 1-hydroxy-1*H*-benzotriazole (0.15 g, 1.12 mmol) were dissolved in CH_2Cl_2 (30 mL). The reaction mixture was stirred at room temperature for three days under a nitrogen atmosphere. The solvent was evaporated, and the product was dissolved in CH_3CN (15 mL). The byproduct urea was removed by filtration, and the filtrate was concentrated under reduced pressure. The crude product was purified by column chromatography with 5% methanol in $CHCl_3$ as the eluent to produce **C** as an orange, foam-like solid; yield 0.27 g (48%); m.p. 270 °C; ^{1}H NMR (400 MHz, $CDCl_3$): δ = 8.55 (d, J = 1.6 Hz, 1H), 8.23 (s, 1H, amide NH), 8.08 (d, J = 2.8 Hz, 1H), 7.83 (dd, J = 8.8, 1.6 Hz, 1H), 7.76 (d, J = 8.8 Hz, 1H), 7.57 (dd, J = 9.2, 2.8 Hz, 1H), 7.56 (d, J = 8.8 Hz, 1H), 7.00 (dd, J = 8.8, 2.0 Hz, 1H), 6.84 (d, J = 2.0 Hz, 1H), 6.70 (d, J = 9.2 Hz, 1H), 6.12 (s, 2H, amine NH_2), 4.27 (t, J = 5.8 Hz, 1H), 3.87 (m, 1H), 3.39 (m, 1H), 2.61 (s, 3H), 2.38 (m, 2H), 2.14 ppm (m, 2H); ^{13}C NMR (100 MHz, [D_6]-dimethylsulfoxide ([D_6]DMSO)): δ = 195.6, 169.9, 144.9, 140.1, 135.0, 129.2, 128.7, 128.2, 127.7, 124.7, 124.2, 123.8, 122.5, 117.0, 115.1, 114.3, 111.1, 104.8, 62.58, 47.87, 29.74, 24.53, 22.24 ppm.

*Synthesis of **ANO1***: Hydrochloric acid (1 mL) was added dropwise to a solution of **C** (0.20 g, 0.48 mmol) in CH_2Cl_2 (10 mL) at 0 °C. The reaction mixture was stirred for 30 min. $SnCl_2{\cdot}2H_2O$ (1.4 g, 6.21 mmol) was added to this mixture, and stirring was continued overnight at room temperature. The resulting mixture was washed with 2N KOH and extracted with CH_2Cl_2. The organic phase was dried over Na_2SO_4, filtered, and evaporated. The crude product was purified by column chromatography with 5% methanol in $CHCl_3$ as the eluent to afford a yellow powder; yield 0.14 g (75%); m.p. 180 °C; ^{1}H NMR (400 MHz, $CDCl_3$): δ = 8.32 (d, J = 1.6 Hz, 1H), 7.96 (s, 1H, amide NH), 7.93 (dd, J = 8.8, 1.6 Hz, 1H), 7.82 (d, J = 9.2 Hz, 1H), 7.65 (d, J = 8.8 Hz, 1H), 7.06 (dd, J = 9.2, 2.4 Hz, 1H), 7.05 (s, 1H), 6.93 (d, J = 2.4 Hz, 1H), 6.55 (s, 2H), 4.25 (t, J = 5.8 Hz, 1H), 3.86 (m, 1H), 3.43 (m, 1H), 3.35 (br s, 4H, diamine 2NH_2), 2.66 (s, 3H), 2.40 (m, 2H), 2.13 ppm (m, 2H); ^{13}C NMR (100 MHz, $CDCl_3$): δ = 197.6, 171.1, 147.2, 137.3, 135.6, 131.7, 131.3, 130.4, 126.6, 126.2, 124.9, 117.2, 116.7, 112.1, 109.3, 107.2, 65.1, 50.2, 31.9, 30.0, 26.8 ppm; HRMS (FAB$^+$): m/z calcd for [$C_{23}H_{25}N_4O_2$]: 389.1978; found: 389.1978.

*Synthesis of **ANO1-T***: Sodium nitrite ($NaNO_2$, 0.25 g, 3.6 mmol) was added dropwise to a mixture of ANO1 (0.14 g, 0.36 mmol) in HCl (aq, pH 2) solution over a period of 30 min at 0 °C. The mixture was stirred for 1 h at room temperature. The crude product was extracted with CH_2Cl_2, washed with water in twice, and evaporated. The residue was purified by column chromatography with ethyl acetate/hexane (4:1) as the eluent to afford a dark yellow, foam-like solid; yield: 0.072 g (51%); m.p. 155 °C; ^{1}H NMR (400 MHz, $CDCl_3$): δ = 8.49 (d, 1H, amide NH), 8.34 (d, J = 1.6 Hz, 1H), 7.95 (dd, J = 8.8, 1.6 Hz, 1H), 7.86 (d, J = 8.8 Hz, 1H), 7.83 (br d, J = 9.2 Hz, 1H), 7.68 (d, J = 8.8 Hz, 1H), 7.10 (dd, J = 8.8, 2.4 Hz, 1H), 7.00 (br s, 1H), 6.98 (d, J = 2.4 Hz, 1H), 4.36 (t, J = 6.0 Hz, 1H), 3.96 (m, 1H), 3.48 (m, 1H), 2.66 (s, 3H), 2.48 (m, 2H), 2.16 ppm (m, 2H); ^{13}C NMR (100 MHz, [D_6]DMSO): δ = 196.6, 172.0, 146.6, 136.9, 130.7, 130.4, 130.0, 125.6, 124.5, 124.0, 116.3, 104.7, 62.18, 48.69, 31.45, 26.42, 23.52 ppm; HRMS (FAB$^+$): m/z calcd for [$C_{23}H_{22}N_5O_2$]: 400.1774; found: 400.1773.

Spectroscopic measurements: Absorption spectra were recorded on a S-3100 UV/Vis spectrophotometer, and fluorescence spectra were obtained with a FluoroMate FS-2 fluorescence spectrophotometer with a 1 cm standard quartz cell. The fluorescence quantum yield was determined by using coumarin 307 ($\Phi = 0.95$ in MeOH) as the reference by the literature method.[41] Reactive oxygen and nitrogen species (100 μM unless otherwise stated) were administered to ANO1 in PBS (pH 7.4) as follows. Nitric oxide (NO) was used from a stock solution (1.9 mM), prepared by purging PBS (0.01 M, pH 7.4) with N_2 gas for 30 min and then with NO (99.5%) for 30 min.[42] HNO was delivered from $Na_2N_2O_3$ (Angeli's salt, Cayman Chemical). It has been reported that Angeli's salt is a precursor of HNO and NO, so Angeli's salt stock solution was made in deoxygenated PBS, which was prepared by purging with argon gas for 30 min, to prevent NO production.[43] Superoxide (O_2^-), nitrite (NO_2^-), and nitrate (NO_3^-) were delivered from KO_2, $NaNO_2$, and $NaNO_3$ (Aldrich), respectively. H_2O_2, *tert*-butylhydroperoxide (TBHP), and hypochlorite (NaOCl) were delivered from 30, 70, and 10% aqueous solutions, respectively. Hydroxyl radicals (˙OH) and *tert*-butoxy radicals (˙O*t*Bu) were generated by the reaction of 1 mM Fe^{2+} with 200 μM H_2O_2 or TBHP, respectively. Sodium peroxynitrite (Cayman Chemical) was prepared in aqueous stock solution in Millipore water.[44]

Solubility of ANO1 in PBS: A small amount of dye was dissolved in DMSO to prepare the stock solutions (1.0×10^{-2} M). The solution was diluted to (6.0×10^{-3}–6.0×10^{-5}) M and added to a cuvette containing PBS (3.0 mL, pH 7.4) by using a microsyringe. In all cases, the concentration of DMSO in buffer was maintained as 0.2%.[28] The plots of the fluorescence intensity against the total amount of dye injected into the cuvette were linear with low dye content and showed downward curvature as more dye was added (Figure S2 in the Supporting Information). The maximum point in the linear region was taken as the solubility. The solubility of ANO1 and ANO1-T in PBS was 4.0 μM.

Measurement of two-photon cross-section: The two-photon cross-section (δ) was determined by using the femtosecond fluorescence measurement technique previously described.[45] ANO1 and ANO1-T (1.0×10^{-6} M) were dissolved in 30 mM PBS (pH 7.4), and the two-photon induced fluorescence intensity was measured at 720–880 nm by using rhodamine 6G as the reference, because the two-photon properties of this compound have been well characterized in the literature.[46] The intensities of the two-photon induced fluorescence spectra of the reference and sample emitted at the same excitation wavelength were determined. The TPA cross-section was calculated by using $\delta = \delta_r(S_s\Phi_r\Phi_r c_r)/(S_r\Phi_s\Phi_s c_s)$, in which the subscripts s and r stand for the sample and reference molecules, the intensity of the signal collected by a CCD detector was denoted as S, Φ is the fluorescence quantum yield, ϕ is the overall fluorescence collection efficiency of the experimental apparatus, the number density of the molecules in solution was denoted as c, and δ_r is the TPA cross-section of the reference molecule.

Cell culture and imaging: Raw 264.7 cells (American Type Culture Collection (ATCC), Manasas, VA, USA) were cultured in Dulbecco's modified Eagle's medium (DMEM, WelGene Inc., Seoul, Korea) supplemented with 10% fetal bovine serum (FBS, WelGene) and penicillin (100 units mL^{-1}). Two days before imaging, the cells were passaged and plated on 0.17 mm delta T dishes (Bioptechs Inc.). The cells were incubated in a humidified atmosphere of CO_2/air (5:95) at 37 °C. For labeling, the growth medium was removed and replaced with Dulbecco's phosphate buffer (DPBS, WelGene) containing calcium and magnesium. The cells were treated with 1 mM ANO1 or ANO1-T (3 μL) in DMSO stock solution (3 μM ANO1, ANO1-T) and then incubated for 30 min. After staining, the cells were washed three times with DPBS and then imaged.

Two-photon fluorescence microscopy: Two-photon fluorescence microscopy images of ANO1- and ANO1-T-labeled cells and tissues were obtained with spectral confocal and multiphoton microscopes (Leica TCS SP2) with ×10, ×40 dry, and ×100 oil objectives (numerical aperture: NA = 0.30, 0.75, and 1.30, respectively). The two-photon fluorescence microscopy images were obtained with a DM IRE2 Microscope (Leica) by exciting the probes with a mode-locked titanium-sapphire laser source (Coherent Chameleon, 90 MHz, 200 fs) set at a wavelength of 750 nm and output power of 1345 mW, which corresponded to approximately 10 mW average power in the focal plane. To obtain images in the 425–575 nm range, internal photomultiplier tubes were used to collect the signals in an 8-bit unsigned 512×512 and 1024×1024 pixels at 800 and 400 Hz scan speeds, respectively.

Photostability: The photostability of ANO1 was determined by monitoring the changes in TPEF intensity with time at three designated positions of ANO1-labeled (3 μM) Raw 264.7 cells chosen without bias. The TPEF intensity remained nearly the same for one hour (Figure 4d), which indicated high photostability.

Detection window: The TPM image of Raw 264.7 cells labeled with 3 μM ANO1 was bright. Moreover, the TP excited-fluorescence (TPEF) spectrum from the white-circled domain in Figure 4a was symmetrical and slightly blueshifted from that measured in PBS, with an emission maximum at approximately 490 nm (Figure 4b). This indicates that the polarity of the probe environment is rather homogeneous and slightly more hydrophobic than that of PBS. Therefore, NO was detected by using a detection window of 425–575 nm. For colocalization experiments, the emission spectra of ANO1 and LysoTracker Red in Raw 264.7 cells were compared. The detection windows for ANO1 and LysoTracker Red were determined by considering two factors: 1) the emission from the two probes should be separated as far as possible and 2) the emission intensities from the probes should be similar. The detection windows that meet the above requirements were 425–525 (ANO1) and 575–660 nm (LysoTracker Red), respectively (Figure S6 in the Supporting Information).

Cell viability: To confirm that the probe couldn't affect the viability of Raw 264.7 cells under the experimental incubation conditions, a CCK-8 kit (Dojindo, Japan) was used according to the manufacturer's protocol. The results are shown in Figure 6.

Effects of LPS, IFN-γ, NMDA, and L-NAME: The stock solution of 10 mM NMDA (Sigma–Aldrich) was prepared by dissolving NMDA (1.5 mg) in distilled H_2O (1.0 mL), and the solution of 100 mM L-NAME (Sigma–Aldrich) was prepared by dissolving L-NAME·HCl (27 mg) in H_2O (1.0 mL). Each solution (1 μL) was diluted to 0.1 mL with artificial cerebrospinal fluid (ACSF; 138.6 mM NaCl, 3.5 mM KCl, 21 mM $NaHCO_3$, 0.6 mM NaH_2PO_4, 9.9 mM D-glucose, 1 mM $CaCl_2$, and 3 mM $MgCl_2$) and added to the imaging solution (0.9 mL) with a micropipette. The stock solution of LPS (Sigma–Aldrich) was prepared by dissolving LPS (1 mg) in DPBS (1.0 mL). The solution (1.25 μL) was diluted into imaging cell medium (1.0 mL). The stock solution of IFN-γ (Sigma–Aldrich) was prepared by dissolving 100 μg of IFN-γ in DPBS (1 mL). The solution was diluted by 10% in DPBS. The final stock solution of IFN-γ (2 μL) was added to the imaging cell medium (1.0 mL).

Preparation and staining of fresh rat hippocampal slices: Slices were prepared from the hippocampi of 2-week-old rats (SD). Coronal slices were cut to 400 μm thick by using a vibrating-blade microtome in ACSF (138.6 mM NaCl, 3.5 mM KCl, 21 mM $NaHCO_3$, 0.6 mM NaH_2PO_4, 9.9 mM D-glucose, 1 mM $CaCl_2$, and 3 mM $MgCl_2$). Slices were incubated with 20 μM ANO1 in ACSF bubbled with CO_2/air (5:95) for 1 h at 37 °C. Slices were then washed three times with ACSF, transferred to 0.17 mm delta T dishes (Bioptechs Inc.), and observed in a spectral confocal multiphoton microscope. The TPM images of fresh rat hippocampal slices labeled with 20 μM ANO1 obtained at 100–180 μm depth are shown in Figure S7 in the Supporting Information.

Acknowledgements

This work was supported by the Korea Healthcare Technology R&D Project, Ministry of Health & Welfare, Republic of Korea (A111182), NRF grants (nos.: 2011-0028663, 2011-0004321, and 2011-0018396), and an Ajou University research fellowship of 2011.

[1] T. Ueno, T. Nagano, *Nat. Methods* **2011**, *8*, 642–645.
[2] D. W. Domaille, E. L. Que, C. J. Chang, *Nat. Chem. Biol.* **2008**, *4*, 168–175.

[3] L. D. Lavis, R. T. Raines, *ACS Chem. Biol.* **2008**, *3*, 142–155.
[4] N. Johnsson, K. Johnsson, *ACS Chem. Biol.* **2007**, *2*, 31–38.
[5] B. N. Giepmans, S. R. Adams, M. H. Ellisman, R. Y. Tsien, *Science* **2006**, *312*, 217–224.
[6] F. Murad, *Angew. Chem.* **1999**, *111*, 1976–1989; *Angew. Chem. Int. Ed.* **1999**, *38*, 1856–1868.
[7] *Nitric Oxide Biology and Pathobiology* (Ed.: L. J. Ignarro), Academic Press, San Diego, CA, **2000**.
[8] S. Moncada, R. M. Palmer, E. A. Higgs, *Pharmacol. Rev.* **1991**, *43*, 109–142.
[9] C. Bogdan, *Nat. Immunol.* **2001**, *2*, 907–916.
[10] P. Pacher, J. S. Beckman, L. Liaudet, *Physiol. Rev.* **2007**, *87*, 315–424.
[11] T. Nagano, T. Yoshimura, *Chem. Rev.* **2002**, *102*, 1235–1270.
[12] H. Kojima, N. Nakatsubo, K. Kikuchi, S. Kawahara, Y. Kirino, H. Nagoshi, Y. Hirata, T. Nagano, *Anal. Chem.* **1998**, *70*, 2446–2453.
[13] H. Kojima, Y. Urano, K. Kikuchi, T. Higuchi, Y. Hirata, T. Nagano, *Angew. Chem.* **1999**, *111*, 3419–3422; *Angew. Chem. Int. Ed.* **1999**, *38*, 3209–3212.
[14] E. Sasaki, H. Kojima, H. Nishimatsu, Y. Urano, K. Kikuchi, Y. Hirata, T. Nagano, *J. Am. Chem. Soc.* **2005**, *127*, 3684–3685.
[15] M. H. Lim, D. Xu, S. J. Lippard, *Nat. Chem. Biol.* **2006**, *2*, 375–380.
[16] M. H. Lim, B. A. Wong, W. H. Pitcock, Jr., D. Mokshagundam, M. H. Baik, S. J. Lippard, *J. Am. Chem. Soc.* **2006**, *128*, 14364–14373.
[17] M. H. Lim, S. J. Lippard, *Acc. Chem. Res.* **2007**, *40*, 41–51.
[18] Y. Yang, S. K. Seidlits, M. M. Adams, V. M. Lynch, C. E. Schmidt, E. V. Anslyn, J. B. Shear, *J. Am. Chem. Soc.* **2010**, *132*, 13114–13116.
[19] E. Tomat, E. M. Nolan, J. Jaworski, S. J. Lippard, *J. Am. Chem. Soc.* **2008**, *130*, 15776–15777.
[20] P. J. Dittmer, J. G. Miranda, J. A. Gorski, A. E. Palmer, *J. Biol. Chem.* **2009**, *284*, 16289–16297.
[21] T. Caporale, D. Ciavardelli, C. Di Ilio, P. Lanuti, D. Drago, S. L. Sensi, *Exp. Neurol.* **2009**, *218*, 228–234.
[22] F. Helmchen, W. Denk, *Nat. Methods* **2005**, *2*, 932–940.
[23] W. R. Zipfel, R. M. Williams, W. W. Webb, *Nat. Biotechnol.* **2003**, *21*, 1369–1377.
[24] G. C. R. Ellis-Davies, *ACS Chem. Neurosci.* **2011**, *2*, 185–197.
[25] B. G. Wang, K. Konig, K. J. Halbhuber, *J. Microsc.* **2010**, *238*, 1–20.
[26] M. D. Cahalan, I. Parker, *Annu. Rev. Immunol.* **2008**, *26*, 585–626.
[27] M. K. Kim, C. S. Lim, J. T. Hong, J. H. Han, H. Y. Jang, H. M. Kim, B. R. Cho, *Angew. Chem.* **2010**, *122*, 374–377; *Angew. Chem. Int. Ed.* **2010**, *49*, 364–367.
[28] H. M. Kim, H. J. Choo, S. Y. Jung, Y. G. Ko, W. H. Park, S. J. Jeon, C. H. Kim, T. Joo, B. R. Cho, *ChemBioChem* **2007**, *8*, 553.
[29] M. Y. Kang, C. S. Lim, H. S. Kim, E. W. Seo, H. M. Kim, O. Kwon, B. R. Cho, *Chem. Eur. J.* **2012**, *18*, 1953–1960.
[30] H. M. Kim, B. R. Cho, *Acc. Chem. Res.* **2009**, *42*, 863–872.
[31] H. M. Kim, B. R. Cho, *Chem. Asian J.* **2011**, *6*, 58–69.
[32] S. Sumalekshmy, C. J. Farhni, *Chem. Mater.* **2011**, *23*, 483–500.
[33] X. Zhang, W. S. Kim, N. Hatcher, K. Potgieter, L. L. Moroz, R. Gillette, J. V. Sweedler, *J. Biol. Chem.* **2002**, *277*, 48472–48478.
[34] X. Ye, S. S. Rubakhin, J. V. Sweedler, *J. Neurosci. Methods* **2008**, *168*, 373–382.
[35] *Calcium Signaling*, 2nd ed. (Ed.: J. W. Putney, Jr.), CRC Press, Boca Raton, FL, **2006**.
[36] *A Guide to Fluorescent Probes and Labeling Technologies*, 10th ed. (Ed.: R. P. Haugland), Molecular Probes, Eugene, OR, **2005**.
[37] E. M. M. Mannders, J. Stap, G. J. Brakenhoff, R. V. Driel, J. A. Aten, *J. Cell Sci.* **1992**, *103*, 857–862.
[38] E. S. Furfine, M. F. Harmon, J. E. Paith, E. P. Garvey, *Biochemistry* **1993**, *32*, 8512–8517.
[39] H. Kojima, N. Nakatsubo, K. Kikuchi, Y. Urano, T. Higuchi, J. Tanaka, Y. Kudo, T. Nagano, *Neuroreport* **1998**, *9*, 3345–3348.
[40] M. L. Pall, *FASEB J.* **2002**, *16*, 1407–1417.
[41] G. A. Crosby, J. N. Demas, *J. Phys. Chem.* **1971**, *75*, 991–1024.
[42] J. H. Shin, B. J. Privett, J. M. Kita, R. M. Wightman, M. H. Schoenfisch, *Anal. Chem.* **2008**, *80*, 6850–6859.
[43] C. Amatore, S. Arbault, C. Ducrocq, S. Hu, I. Tapsoba, *ChemMedChem* **2007**, *2*, 898–903.
[44] M. D. Pluth, L. E. McQuade, S. J. Lippard, *Org Lett.* **2010**, *12*, 2318–2321.
[45] S. K. Lee, W. J. Yang, J. J. Choi, C. H. Kim, S.-J. Jeon, B. R. Cho, *Org. Lett.* **2005**, *7*, 323–326.
[46] N. S. Makarov, M. Drobizhev, A. Rebane, *Optics Express* **2008**, *16*, 4029–4047.

Received: April 9, 2012
Revised: June 21, 2012
Published online: ■■ ▮▮, 0000

Fluorescent Probes

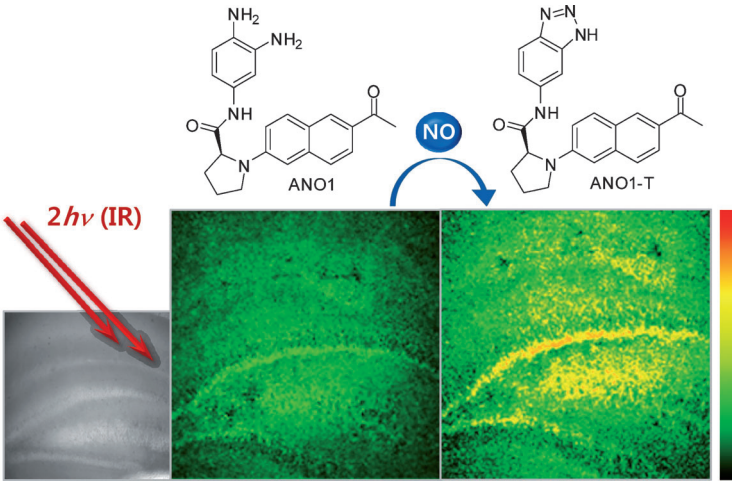

NO lightens up: A small-molecule two-photon (TP) probe (ANO1; see scheme) is reported that shows a rapid and specific nitric oxide (NO) response, in the form of a strong TP excited-fluorescence enhancement in response to NO, with a maximum TP-action cross-section of 170 GM (GM: 10^{-50} cm^4 photon^{-1}). The probe can be easily loaded into cells and can real-time monitor NO in living tissues.